Proceedings of NUMOS
Gent, 28-30 March 2007

Numos 2007, pp. 327–339

Modelling MEH-PPV:PCBM (1:4) bulk heterojunction solar cells

Ben Minnaert and Marc Burgelman

University of Gent, Electronics and Information Systems (ELIS)
Pietersnieuwstraat 41, B-9000 Gent, Belgium.

Abstract

Basic solar cell characteristics were examined in an organic bulk heterojunction device. The active layer is a spincoated organic blend of a *p*-material (MEH-PPV) and an *n*-material (the fullerene derivative PCBM), sandwiched between a transparent ITO-PEDOT/PSS electrode and an Al/LiF back-contact. We carried out light and dark *I-V* and spectral response measurements and measured the transparency of the active layer. Modelling of organic bulk-heterojunction solar cells is difficult because of the complicated geometry and because of the microscopic scale of the internal mechanisms. We applied an effective medium model in which the whole *p-n* nanostructure is represented by one single effective semiconductor layer, which then is fed into a standard solar cell device simulator, e.g. SCAPS. First, a parameter set was built up that simulates the measured characteristics of the MEH-PPV / PCBM blend cells. The dark and illuminated *I-V*, and the spectral response measurements are fitted fairly well. A parameter set for the effective medium model was sought and found that describes (with qualitative agreement) the measured *I-V* curves. This parameter was then used for a numerical parameter study. Critical issues for cell performance were identified, and their influence quantified (based on the actual parameter set for MEHPPV-PCBM cells). First, the cell performance is sensitive to the electron and hole mobilities in the materials: the efficiency increases monotonously with increasing mobility, over many decades. The sensitivity is about 25 % relative efficiency gain for an order of magnitude of increase of the mobilities. Second, the poor absorption of the solar illumination is a cause of weak performance. We investigated the influence on cell thickness, and of the absorption characteristic.

1. Introduction

Photovoltaic solar cells based on conjugated polymer/fullerene compounds are promising candidates for solar energy conversion. Organic plastic cells have the potential for cost effectiveness and mechanical flexibility. A bulk heterojunction solar cell consist of a interpenetrating network of an *n*-type (e.g. fullerene derivatives) and a *p*-type (semi)conductor (e.g. conjugated

polymer), sandwiched between two electrodes with different work functions [1].

On one substrate, five bulk heterojunction solar cells with a different area were made. The active layer is a spin coated organic blend of a *p*- and *n*-material, respectively the polymer poly(2-methoxy-5(2'-ethyl-hexyloxy)-1,4-phenylenevinylene (MEH-PPV) and the fullerene derivative [6,6]-phenyl-C_{61}-butyric acid methyl ester (PCBM), in a 1:4 weight ratio. Glass plates covered with a 100 nm thick layer of Indium Tin Oxide (ITO) with a sheet resistance of around 14 Ω / square are purchased from Merck Display Technologies and diced into 5 cm × 5 cm substrates. The ITO forms a good front contact with a transmission of around 90 % in the visible range. The glass substrates are cleaned in an ultrasonic bath of acetone and afterwards in boiling isopropanol (IPA). By using photolithography, part of the ITO is etched away to form 5 different tracks for the 5 front contacts. After again cleaning in an ultrasonic acetone bath and boiling IPA, an oxygen plasma treatment is done to (i) clean the substrate, (ii) improve the properties of the ITO and (iii) make the surface hydrophilic to facilitate the deposition of PEDOT/PSS.

A layer of PEDOT/PSS (Baytron P, HP Starck) is spin coated to a thickness of 100 nm on top of the ITO from an aqueous dispersion, giving a conductive layer (≈ 10^{-3} S/cm) that prevents shorts and improves the diode behaviour [2,3]. The photoactive layer consisting of MEH-PPV:PCBM (1:4 by weight ratio) is spin coated on top of the PEDOT to a thickness of 100 nm (+/- 10 nm) from solution. Because organic π-conjugated semiconductors like MEH-PPV are known for their rapid degradation under combined exposure to light and oxygen, the spin coating is done in a nitrogen atmosphere.

For the negative back contact, a two-layer deposition is performed through a shadow mask. First, a small amount of LiF is thermally deposited onto the active layer with a thickness of about 1 nm to increase the fill factor (*FF*) and the short circuit voltage V_{oc} [1,4]. In the second step, Al is thermally evaporated to a thickness of 100 nm. The geometrical overlap between the positive electrode ITO and the negative electrode LiF/Al defines the active area. The tracks of LiF/Al are deposited perpendicular on the ITO-tracks in such a way that 5 active areas (i.e. 5 bulk heterojunction solar cells) originate on 1 substrate (2 cells with an active area of 3 mm × 3 mm, 2 cells of 5 mm × 5 mm, and 1 cell of 7 mm ×7 mm). Because of the instability to light and oxygen, the device must be sealed. This is done in a nitrogen atmosphere by putting a glass cover plate over the back contact, making external contacts with metal bands and sealing the whole with a spacer and epoxy.

2. Measurements

We performed current–voltage (*J-V)* measurements with bias voltage varying between -2 V an 2 V. Positive bias is defined as positive voltage to the ITO-contact. The *J-V* curves are taken both in the dark and in the light under simulated solar illumination (AM 1.5-spectrum, 100 mW/cm²).

2.1 Analysis of the dark *J-V* characteristics

From the dark *J-V* characteristics rectification ratios of 10^3 at 2 V are achieved for the cells with an active area A of 9 mm² and ratios of 10^2 for the cells of 25 mm² and 49 mm². Usually, this large ratio is attributed to the interfacial layer of PEDOT/PSS at the ITO-contact [2].

Table 1 Fitting parameters of the phenomenological model of Eq. (1) to the dark *J-V* measurement of an MEH-PPV:PCBM (1:4) bulk heterojunction cell with an active area of 9 mm².

Parameter	Symbol	Value	Unit
series resistance (discrete)	$R_s.A$	113	Ωcm^2
shunt resistance	$R_{sh}.A$	$8\ 10^5$	Ωcm^2
shunt conductance	G_{sh}/A	$1.25\ 10^{-6}$	Scm^{-2}
main cell diode			
saturation current	J_1	$1.39\ 10^{-15}$	Acm^{-2}
ideality factor	n_1	1.30	
power law diode			
exponent	n_2	2.50	
reference current	J_2	$8\ 10^{-7}$	Acm^{-2}
reference voltage	V_2	0.50	V

The dark characteristics cannot be fitted to an ideal Shockley diode equation in the whole voltage. The addition of series resistance is necessary to obtain a good fit for $V > 0.8$ V. A shunt resistance is necessary to get a good fit for $|V| < 0.2$ V. With these parasite components, the main diode, this is a Shockley diode with ideality factor $n_1 = 1.3$, still gives only a good fit in the voltage range from 0.6 V to 0.8 V. For intermediate forward voltages between 0.2 V and 0.6 V, we need to introduce a second diode, which is in this case described by a power law, and not by an exponential Shockley law. So the dark *J-V* characteristics are fitted to:

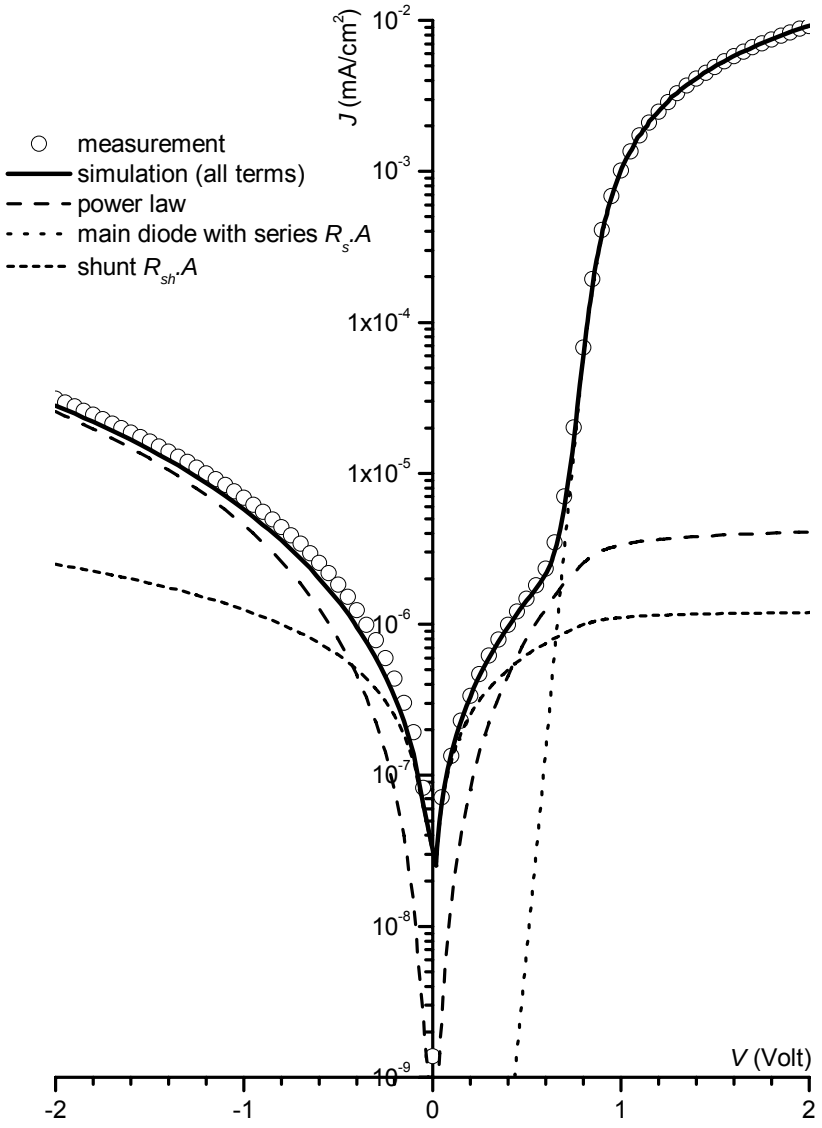

Figure 1 Dark *J-V* measurement of an MEH-PPV:PCBM (1:4) bulk heterojunction cell with an active area of 9 mm² (open circles; only one measurement point out of five is shown). The fitting of these curves to the phenomenological model of Eq. (1), with the parameters of Table 1, is shown in a solid line, the separate terms of Eq. (1) are shown in dashed or dotted line style (see inset).

$$J = J_1\left[\exp\left(\frac{q\left(V - R_s J\right)}{n_1\, kT}\right) - 1\right] + G_{sh}\left(V - R_s J\right) + J_2\left(\frac{V}{V_2}\right)^{n_2} \tag{1}$$

The parameter values J_1, n_1,J_2, V_2, n_2, R_s and G_{sh} are listed in Table 1, and the measurement and the fitted curve are shown in Figure 1.

When the analysis is done for different cells on one substrate, one can attribute the total series resistance R_sA to an internal contribution $R_{\text{int}}.A$ and an external one, coming from the ITO conductor path. The external R_sA has a discrete R_s-part (from the ITO path from the cell to the substrate edge) and a distributed R_s-part (from the ITO covering the cell):

$$R_s \cdot A = R_{\text{int}} a^2 + R_{\square}\left(\frac{a^2}{3} + aL\right) = R_{\text{int}} a^2 + R_{\square} a\left(L + \frac{a}{3}\right) \tag{2}$$

with a the cell width, L the length of the ITO-path and $R_{\square}$ the sheet resistance of the ITO (see Figure 2). The resistance of the n-contact Al is negligible.

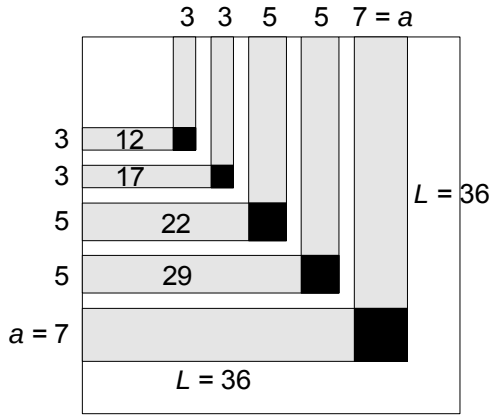

Figure 2 Layout of the different cells on the same substrate, and definition of cell width a and the length L of the ITO-path (all dimensions in mm). The horizontal paths are e.g. ITO, and have a sheet resistance $R_{\square}$; the vertical ones are aluminium (Al), and are supposed to have no resistance.

The comparison between measurement and calculation can be found in Figure 3, with $R_{\square}$ = 14 Ω and $R_{\text{int}}.A$ = 11 Ωcm^2. The measurements should be corrected for the external series resistance before physical modelling of its characteristics.

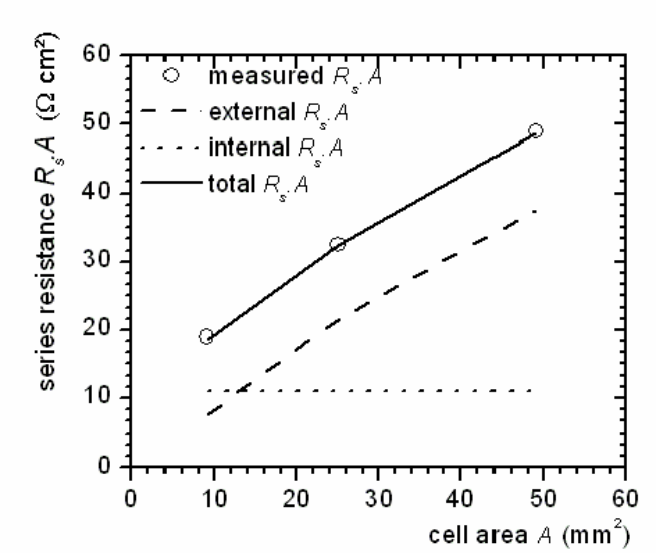

Figure 3 Measured R_sA values (open circles), and calculated R_sA, with Eq. (2), with the geometry parameters a and L, $R_{\square}$ = 14 Ω and $R_{int}.A$ = 11 Ωcm^2. The two contributions to R_sA, i.e. the external and internal series resistance, are shown separately.

2.2 Analysis of the illuminated *J-V* characteristics

The cells have an efficiency of 1.3 % under simulated solar illumination (AM 1.5-spectrum, 100 mW/cm²). The other characteristics of the illuminated solar cells are given in Table 2.

Table 2 Characteristics of the illuminated MEH-PPV / PCBM cells (AM 1.5-spectrum, 100 mW/cm²), and the solar cell performance parameters J_{sc}, V_{oc} , FF and η.

Property	Symbol	Unit	Value		
area	A	mm^2	9	25	49
short circuit current density	J_{sc}	mA/cm^2	3.62	3.69	3.49
open circuit voltage	V_{oc}	V	861	860	854
fill factor	FF	%	44.1	41.5	40.4
efficiency	η	%	1.38	1.32	1.21

The *J-V* curves of cells with different area are shown in Figure 4.

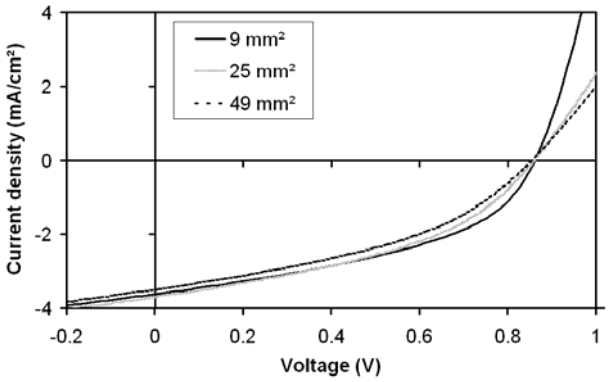

Figure 4 *J-V* characteristics under illumination (AM 1.5-spectrum, 100 mW/cm²) of MEH-PPV:PCBM (1:4) bulk heterojunction cells with an active area of 9 mm², 25 mm² and 49 mm².

Table 2 and Figure 4 show that the fill factor *FF* of the cell decreases with increasing active area *A*. This effect is also reflected by the fact that the current reduces with increasing surface area *A* for voltages above V_{oc}. which is clearly visible on Figure 4. The reason of these two observations is the increase of series resistance R_sA. This increase was shown in the previous paragraph, and could be attributed to the increase in path of the ITO, which has a high sheet resistance $R_{\square}$.

2.3 The quantum efficiency

The external quantum efficiency (*EQE*) was measured in function of the wavelength (Figure 5). Also the specular transmission $T(\lambda)$ in function of the wavelength of the layer ITO/PEDOT/MEH-PPV:PCBM was measured. The internal quantum efficiency (*IQE*) was calculated by dividing the *EQE* by (1-*T*). This results in an approximation of the *IQE* (the reflection was neglected). Most of the absorption happens in the small band 380 nm – 570 nm. This spectral response is not well matched to the spectrum of the sun. About 50 % of the power in the AM1.5 spectrum has a wavelength longer than 685 nm. This obviously limits the ultimate efficiency obtainable from a device based on MEH-PPV and PCBM.

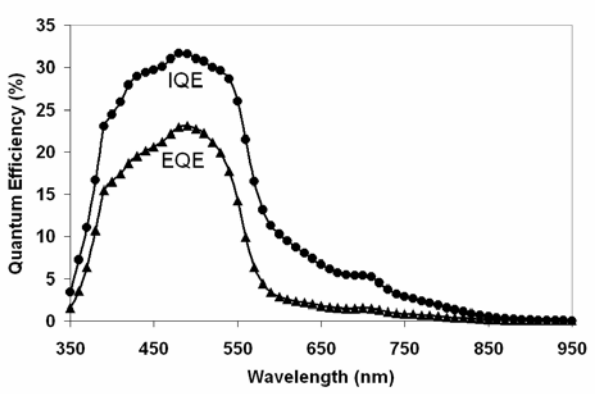

Figure 5 External and internal quantum efficiency in function of the wavelength of an MEH-PPV:PCBM (1:4) bulk heterojunction cell with an active area of 9 mm².

3. Modelling of measured cells

3.1 The effective medium model

In the effective medium model (EMM), the whole *p*-*n* nanostructure is represented by one single effective medium layer [5,6]. We consider selective contacts, i.e. one contact only accepts electrons, the other one only accepts holes. This creates the driving force for the separation of generated electron-hole pairs in the effective medium. The effective medium is characterized by an "averaging" of the properties of the *n*- and the *p*-material. The effective medium has one conduction band namely the conduction band of the *n*-type material or the lowest unoccupied molecular orbital (LUMO) of the acceptor molecule in a bulk heterojunction solar cell. The effective medium has also one valence band namely the valence band of the *p*-type material or the highest occupied molecular orbital (HOMO) of the donor molecule in a bulk heterojunction solar cell (Figure 6). This configuration is then fed into a standard solar cell device simulator, e.g. SCAPS [7]. Also other carrier related properties of the effective medium semiconductor are given by the corresponding material: the mobility μ_n, the diffusion constant D_n, the effective density of states N_C of the conduction band are those of the *n*-material, whilst the values of μ_p, D_p, N_V are those of the *p*-material. Non-carrier related properties, such as the dielectric constant ε, the refractive index n, and the absorption constant α are influenced by both materials. The precise way in which this happens depends strongly on the details and the size scale of the intermixing. Notice that in the effective medium, the intermediate step where excitons are created and dissociated is lost.

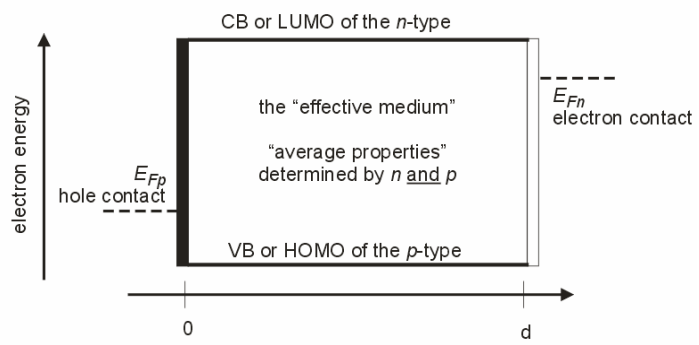

Figure 6 Schematics of the effective medium model. The intimate blend of an *n*-type material and a *p*-type material is represented by one single 'effective' material with 'average' properties.

3.2 Numerical parameter study

We now apply the EMM to the MEH-PPV / PCBM organic bulk heterojunction. First, a parameter set was built up. The main parameters are listed in Table 3, and are explained here in brief.

The dielectric constant ε_s then comes from a capacitance measurement. The cell thickness d comes from measurement. The absorption constant $\alpha(\lambda)$ was calculated from the thickness d and the absorption A, where A was simply taken as $A(\lambda) = 1 - T(\lambda)$, with $T(\lambda)$ the measured transmission. The work functions Φ_{m1} and Φ_{m2} of the electrode materials come from literature [8][9]. The electron affinity χ of the effective medium (EM) is determined by the LUMO level of the *n*-type constituent of the EM, thus the PCBM, which is taken from literature [10]. The value of $\chi + E_g$, where E_g is the band gap of the EM, is determined by the HOMO of the *p*-type constituent of the EM, thus the MEH-PPV, which is taken from literature [11]. Since the parameters Φ_{m1}, Φ_{m2}, χ and E_g can depend slightly on technological modifications, we allowed for some slight variation in the fitting procedure. The mobility μ_n of the EM is the electron mobility of the *n*-type constituent of the EM, and the mobility μ_p of the EM is the electron mobility of the *p*-type constituent of the EM. The mobilities measured on FET-structures [12] are taken as first guesses, and then adapted in the fitting procedure.

The EMM with this parameter set was fed into the solar cell simulation package SCAPS [7], and the parameters were adapted to obtain a reasonable fit with the measured characteristics of the MEH-PPV / PCBM blend cells, i.e. the dark and illuminated *J-V*, and the spectral response $QE(\lambda)$ measurements.

Table 3 Main parameters of the standard parameter set for a MEH-PPV / PCBM with surface area 25 mm².

Parameter	Symbol	Value	Unit
p-contact: ITO / PEDOT-PSS			
work function	Φ_{m1}	4.7	eV
n-contact: Al / LiF			
work function	Φ_{m2}	4.3	eV
effective medium: MEH-PPV / PCBM			
thickness	d	100	nm
band gap	E_g	1.25	eV
electron affinity	χ	3.75	eV
electron mobility	μ_n	$2\ 10^{-3}$	$cm^2V^{-1}s^{-1}$
hole mobility	μ_p	$2\ 10^{-4}$	$cm^2V^{-1}s^{-1}$
dielectric constant (relative)	ε_s	3	
maximum absorption constant	α_{max}	$2.6\ 10^4$	cm^{-1}
wavelength of max. absorption	λ_{max}	495	nm

This parameter set was then used for a numerical parameter study.

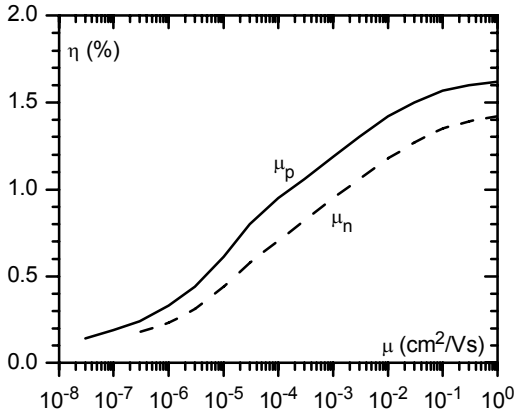

Figure 7 Calculated influence of the mobilities μ_p and μ_n of the *p* and *n* material on the efficiency η. When one mobility was varied, the value of the other mobility, and of all other parameters is taken from the standard parameter set for the MEH-PPV cell, see Table 3.

Critical issues for cell performance are identified, and their influence quantified (based on the actual parameter set for MEH-PPV / PCBM cells).

First, the cell performance is sensitive to the mobilities μ_n and μ_p in the materials: the efficiency η increases monotonously with increasing μ, over many decades (Figure 7). The sensitivity is about 25% relative efficiency gain for an order of magnitude of increase of the mobilities.

Second, the poor absorption of the solar illumination is a cause of weak performance. We investigated the influence on cell thickness *d* (Figure 8), and of the absorption characteristic $\alpha(\lambda)$. Making thicker cells is a technological problem, and not attractive from the fabrication viewpoint. Developing materials with smaller bandgap, and a broader absorption $\alpha(\lambda)$ is a subject of active actual research [9]. Organic materials show a more narrow absorption $\alpha(\lambda)$ than inorganic semiconductors. A broader effective use of the solar spectrum can be obtained by combining organic materials with different band gap in a multi-junction structure.

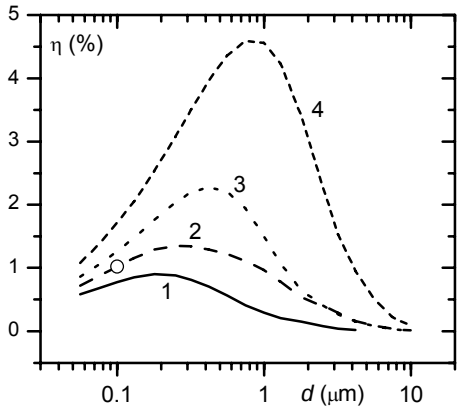

Figure 8 Calculated influence of the cell thickness *d* on the efficiency η: curve 1: $\mu_n = \mu_p = 2\ 10^{-4}$, curve 2: standard parameter set (Table 3); curve 3: $\mu_n = \mu_p = 2\ 10^{-3}$ and curve 4: $\mu_n = \mu_p = 2\ 10^{-2}$, all in units of cm^2/Vs. The actual cell measurement, corresponding to the standard parameter set, is indicated with a circle.

4. Conclusions

Light and dark *I-V*, spectral response and transparency measurements were carried out in an MEH-PPV:PCBM (1:4) bulk heterojunction cell. We applied an effective medium model by building up a parameter set that simulates the measured characteristics. With the standard solar cell device simulator SCAPS, we identified and quantified critical issues for cell performance, that is the mobilities, the cell thickness and the absorption.

Acknowledgements

The IWT-SBO-project 030220 “Nanosolar”. The cells were made at IMEC, Leuven, Belgium by Tom Aernouts, in the framework of Nanosolar.

References

[1] C.J. Brabec, “Semiconductor aspects of organic bulk heterojunction solar cells”, in *Organic Photovoltaics: Concepts and Realization*, C.J. Brabec, V. Dyakonov, J. Parisi and N. Sariciftci (editors), Springer, Chapter 5, pp. 214-221, 2003.

[2] W. Geens, T. Aernouts, J. Poortmans and G. Hadziioannou, Organic co-evaporated films of a PPV-pentamer and C60: model systems for donor/acceptor polymer blends, *Thin Solid Films*, **403-404**, 438-444 (2002).

[3] T. Aernouts, W. Geens, J. Poortmans, P. Heremans, S. Borghs and R. Mertens, Extraction of bulk and contact components of the series resistance in organic bulk donor-acceptor-heterojunctions, *Thin Solid Films*, **403-404**, 297-301 (2002).

[4] C. J. Brabec, S. E. Shaheen, T. Fromherz, F. Padinger, J. C. Hummelen, A. Dhanabalan, R.A. J. Janssen and N.S. Sariciftci, Organic photovoltaic devices produced from conjugated polymer / methanofullerene bulk heterojunctions, *Synthetic Metals*, **121**, 1517-1520 (2001).

[5] B. Minnaert, C. Grasso and M. Burgelman, An effective medium model versus a network model for nanostructured solar cells, *Comptes Rendus Chimie*, **9**, 735-741 (2006).

[6] M. Burgelman, B. Minnaert, C. Grasso, “Device Modeling of Nanostructured Solar Cells”, in *Nanostructured Materials for Solar Energy Conversion*, T. Soga (editor), Elsevier, Amsterdam, Chapter 2, pp. 45-80, 2006.

[7] M. Burgelman, P. Nollet and S. Degrave, Modelling polycrystalline semiconductor solar cells, *Thin Solid Films*, **361-362**, 527-532 (2000).

[8] C. Brabec, A. Cravino, D. Meissner, N.S. Sariciftci, T. Fromherz, M. Rispens, L. Sanchez and J. Hummelen, Origin of the Open Circuit Voltage of Plastic Solar Cells, *Adv. Funct. Mater.*, **11**, 374-380 (2001).

[9] C. Winder and N. S. Sariciftci, Low bandgap polymers for photon harvesting in bulk heterojunction solar cells, *J. Mater. Chem.*, **14**, 1077-1086 (2004).

[10] S. Sensfuss, M. Al-Ibrahim, A. Konkin, G. Nazmutdinova, U. Zhokhavets, G. Gobsch, D.A.M. Egbe, E. Klemm and H.K. Roth, Characterisation of potential donor acceptor pairs for polymer solar cells by ESR, optical and electrochemical investigations, Proceedings of SPIE (San Diego, August 2003), Vol. 5215, pp. 129-140, Bellingham, Washington, 2004.

[11] S.A. McDonald, P.W. Cyr, L. Levina and E.H. Sargent, Photoconductivity from PbS-nanocrystal/semiconducting polymer composites for solution-processible, quantum-size tunable infrared photodetectors, *Appl. Phys. Lett.*, **85**, 2089-2091 (2004).

[12] W. Geens, S.E. Shaheen, C.J. Brabec, J. Poortmans and N.S. Sariciftci, Field-effect mobility measurements of conjugated polymer/fullerene photovoltaic blends, AIP Conference Proceedings (Kirchberg, Austria, November 2000), Vol. 544, pp. 516-520, New York, 2000.